DOI: http://dx.doi.org/10.12989/cac.2012.10.3.259

Reinforced concrete corbels strengthened with carbon fiber reinforced plastics

Wen-Yao Lu*[1], Hsin-Wan Yu[2], Chun-Liang Chen[3],
Tzong-Hwan Yang[3] and Yu-Sin Lin[3]

[1]*Department of Interior Design, China University of Technology, Taipei 11695, Taiwan, R.O.C.*
[2]*Department of Civil Engineering and Hazard Mitigation Design, China University of Technology, Taipei 11695, Taiwan, R.O.C.*
[3]*Department of Interior Design, China University of Technology, Taipei 11695, Taiwan, R.O.C.*

(Received August 11, 2011, Revised March 21, 2012, Accepted March 24, 2012)

Abstract. A total of nine reinforced concrete corbels were tested, in this study. Six were externally strengthened with carbon fiber reinforced plastics (CFRP), in the horizontal direction. The cross-sectional area of CFRP and the shear span-to-effective depth ratios are the parameters considered, in this study. Test results indicate that the higher the cross-sectional area of CFRP, the higher is the shear strength of the corbels, and the lower the shear span-to-effective depth ratios, the higher is the shear strength of corbels. The shear strength predicted by the design provisions in section 11.8 of the ACI Code, the strut-and-tie model in Appendix A of the ACI Code, and the softened strut-and-tie (SST) model were compared with the test results. The comparisons show that both the strut-and-tie model in Appendix A of the ACI Code, and the SST model can accurately predict the shear strength of reinforced concrete corbels, strengthened with CFRP.

Keywords: reinforced concrete corbel; shear strength; carbon fiber reinforced plastics (CFRP).

1. Introduction

Corbels are brackets that project from the faces of columns. They are used extensively, in precast concrete construction, to support primary beams and girders (Hwang *et al*. 2000). Owing to the prevalence of precast concrete, the use of corbels is a common construction feature (Lu and Lin 2009). Corbels are short cantilevers that generally have shear span-to-effective depth ratios of less than unity. Assessments of the strength of corbels with such a small shear span-to-effective depth ratio are dominated by consideration of shear.

Although the experimental database is extensive for reinforced concrete members strengthened, in flexure, with fiber reinforced plastics composites (FRP), further investigations in the domain of shear strengthening are imperative (Wong and Vecchio 2003). The application of circumferential wrapping FRP as a new technique for external confinement and strengthening of reinforced concrete columns have been used in recent years (Elwan and Rashed 2011). According to a study of the shear strengthening of reinforced concrete beams (Shuraim 2011), carbon fiber reinforced plastics (CFRP) strengthened beams provide an increase in ultimate strength compared to non-strengthened beams.

* Corresponding author, Professor, E-mail: luwenyao@cute.edu.tw

Previous experimental investigations (Kriz and Raths 1965, Mattock *et al.* 1976, Fattuhi and Hughes 1989, Her 1990, Yong and Balaguru 1994, Fattuhi 1994, Foster *et al.* 1996, Lu and Lin 2009) focused on corbels that were not strengthened with CFRP. It is believed that the shear strength of corbels can be enhanced using external CFRP strengthening, but very few, if any, corbels that are externally strengthened with CFRP have been studied. Further experimental work on corbels strengthened with CFRP is necessary.

The shear strength of corbels that are not strengthened with CFRP was accurately predicted by Hwang *et al.* (2000), Russo *et al.* (2005) and Lu *et al.* (2009). In this study, experimental results are presented and then the analytical method for prediction of the shear strength of corbels, externally strengthened with CFRP, is proposed.

2. Experimental study

In this study, nine corbels were tested, under a vertical load. Six were externally strengthened with CFRP, in the horizontal direction. Variables examined, in the tests, are the shear span-to-effective depth ratio and the number of CFRP layers.

2.1 Specimen details

Each specimen consisted of a 320-mm-long column, with two corbels projecting from the column, in a symmetrical fashion (Fig. 1). The 2-#4 primary reinforcement of corbels consisted of parallel straight bars, welded to the steel plates (150 × 50 × 4 mm) at the ends of the corbels, to prevent local bond failures, as shown in Fig. 1. The shear span (a) was measured, from the center of the support to the face of the column (Fig. 1). Two steel plates (150 × 50 × 2 mm) were embedded in the corbels, to prevent bearing failures during the test.

As shown in Table 1, each corbel in this study had a width (b) of 150 mm, an overall depth (h) of 150 mm and an effective depth (d) of 125 mm. The corbel notation, given in Table 1, includes three parts. The first part refers to the compressive strength of concrete, L for low compressive strength concrete. The second part refers to the number of CFRP layers, O, for corbels not strengthened with

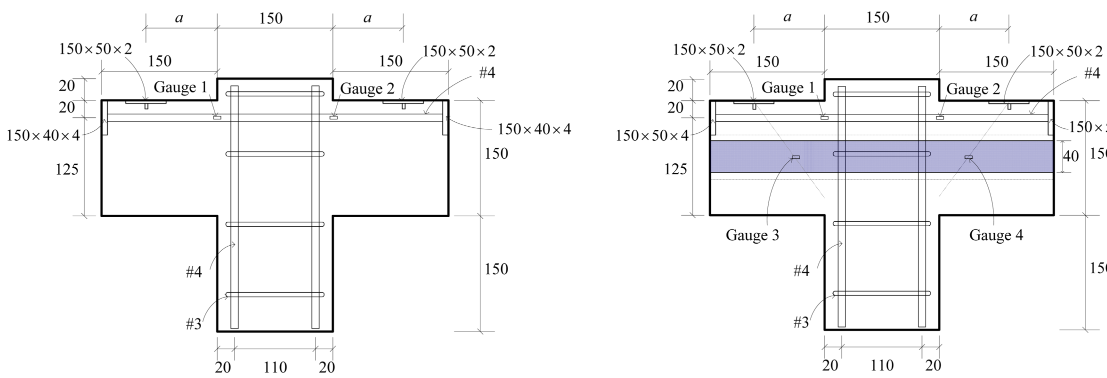

(a) Not strengthened (b) CFRP wrapping in the horizontal direction

Fig. 1 Typical specimen

Table 1 Specimen details

Specimen	f_c' MPa	b mm	d mm	h mm	a mm	a/d	Primary reinforcement	Number of CFRP layers
LO5	25.88	150	125	150	50	0.40	2-#4	0
LA5	25.88	150	125	150	50	0.40	2-#4	4
LB5	25.88	150	125	150	50	0.40	2-#4	6
LO8	25.88	150	125	150	80	0.64	2-#4	0
LA8	25.88	150	125	150	80	0.64	2-#4	4
LB8	25.88	150	125	150	80	0.64	2-#4	6
LO11	25.88	150	125	150	110	0.88	2-#4	0
LA11	25.88	150	125	150	110	0.88	2-#4	4
LB11	25.88	150	125	150	110	0.88	2-#4	6

Table 2 Properties of reinforcement

No.	d_b (mm)	A_b (mm^2)	f_y (MPa)	f_u (MPa)	Remark
#3	9.53	71.33	386.2	535.8	Ties of column
#4	12.70	126.68	386.4	560.8	Primary reinforcement of corbel, Main bars of column

Table 3 Properties of concrete

Design strength	Mean strength	Water-cement ratio	Slump	Coarse aggregate	Unit weight
20.67 MPa	25.88 MPa	0.50	180 mm	20 mm	2387 kg/m^3

Table 4 Properties of CFRP

Tensile strength (MPa)	Thickness (mm)	Modulus of elasticity (MPa)	Unit weight (g/m^2)	ε_u
3900	0.166	230000	300	0.015

CFRP, *A*, for corbels strengthened with 4 layers of CFRP, in the horizontal direction, and *B*, for corbels strengthened with 6 layers of CFRP, in the horizontal direction. The third part signifies the shear span of the corbels, e.g. 5 for shear span a = 5 cm = 50 mm (Table 1).

The yield strength (f_y) and ultimate tensile strength (f_u) of #3 reinforcement are 386.2 MPa and 535.8 MPa, while the yield strength and ultimate tensile strength of #4 reinforcement are 386.4 MPa and 560.8 MPa (Table 2). The properties of the concrete used in this study are shown in Table 3. The design strength of the concrete is 20.67 MPa, but the mean strength of the concrete is 25.88 MPa (Table 3). Table 4 shows that the tensile strength of CFRP is 3900 MPa, the thickness of each layer of carbon fiber sheet is 0.166 mm and the modulus of elasticity is 230000 MPa.

To avoid premature failure of the CFRP material, caused by shearing at sharp corners, the corners of specimens were rounded off, as smoothly as possible. This study used the procedures proposed by Li *et al.* (2003) for wrapping the CFRP around the concrete cylinder. A thin layer of primer epoxy was firstly applied to the concrete surface of the test corbels. After the primer epoxy, on the concrete surface, had cured at the ambient temperature, for two hours, the carbon fiber sheet was

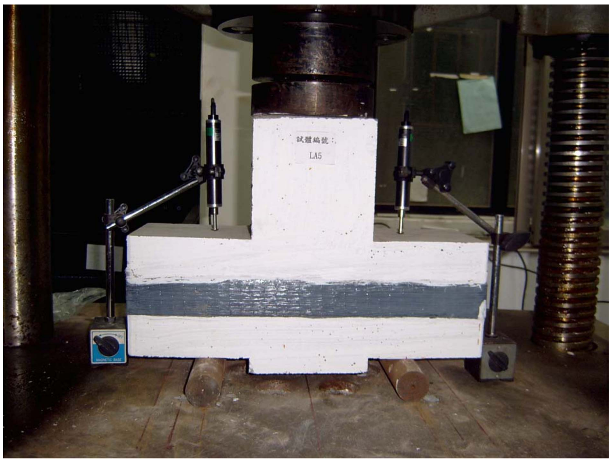

Fig. 2 Testing arrangements for corbels

affixed to the concrete surface, in the horizontal direction (Fig. 1(b)). For each layer of carbon fiber sheet, two plies of epoxy were applied, one on the concrete surface, prior to affixing the sheet and the other on top of the affixed sheet. A paintbrush was used to fully saturate the carbon fiber with epoxy. The extra epoxy in each layer was squeezed out, by compressing the upper surface with a flat plastic scraper (Li *et al.* 2003). After the wrapping procedures were completed, the CFRP were cured, in ambient conditions for more than seven days (Li *et al.* 2003).

2.2 Testing procedures

During the test, the strains in the primary reinforcement were measured, using electrical resistance gauges, 1 and 2 (Fig. 1(a)). For the specimens with CFRP wrapping, in the horizontal direction (Fig. 1(b)), the strains in the CFRP were measured, using electrical resistance gauges, 3 and 4. Prior to testing, both surfaces of the corbels were whitewashed, to aid the observation of crack development, during the test. For convenience, the specimens were tested in an inverted position, as may be seen in Fig. 2. The vertical load was applied to each corbel through the column using a 1000 kN capacity universal testing machine. The corbels, seated on two roller supports, were subjected to upward shear forces against the vertical load. The displacements of the corbels, caused by the shear forces, were measured, using two linear variable differential transformers (LVDTs), as may be seen in Fig. 2. For each load increment, the test data were captured by a data logger and automatically stored.

2.3 Test results

The measured shear strengths of the corbels, $V_{cv,test}$, for each specimen, obtained in the tests, is summarized in Table 5. The test results for corbels with shear span-to-effective depth ratios (a/d) of 0.4 and 0.64 revealed that the shear strength of the corbels increases, as the cross-sectional area of CFRP (A_{CFRP}) increases. However, the effect of A_{CFRP}, on the shear strength of corbels, was not obvious, for the condition $a/d = 0.88$ (Table 5). It is believed that the larger the shear span-to-effective depth ratio of the corbel, the smaller is the effectiveness of the CFRP wrapping, in the

Table 5 Test results

Specimen	a/d	A_{CFRP} (mm^2)	P_u (kN)	$V_{cv,test}$ (kN)	Strain in the primary reinforcement of corbels at ultimate state
LO5	0.40	0	269.50	134.75	4115×10^{-6}
LA5	0.40	53.12	289.1	144.55	2920×10^{-6}
LB5	0.40	79.68	309.68	154.84	4134×10^{-6}
LO8	0.64	0	196.00	98.00	2062×10^{-6}
LA8	0.64	53.12	225.40	112.70	2011×10^{-6}
LB8	0.64	79.68	263.62	131.81	4589×10^{-6}
LO11	0.88	0	191.59	95.80	3799×10^{-6}
LA11	0.88	53.12	179.38	89.69	2169×10^{-6}
LB11	0.88	79.68	198.46	99.23	3754×10^{-6}

horizontal direction. Further experimentation with CFRP wrapping, in the vertical direction, for corbels with a larger shear span-to-effective depth ratio, is necessary, in the future. The results also show that the shear strength of the corbels increases, as the shear span-to-effective depth ratio decreases (Table 5). It can be seen that the strain in the primary reinforcement is beyond the yielding strain of reinforcing bars at ultimate state.

The load-displacement relationship, observed for the corbels, is shown in Fig. 3. For corbels with $a/d = 0.4$, the greater the A_{CFRP}, the greater are the ultimate load and displacements. However, for corbels with $a/d = 0.64$ and 0.88, the effect of CFRP on the load-displacement relationship is not obvious (Fig. 3). CFRP wrapping, in the horizontal direction, for corbels with $a/d = 0.4$ has a

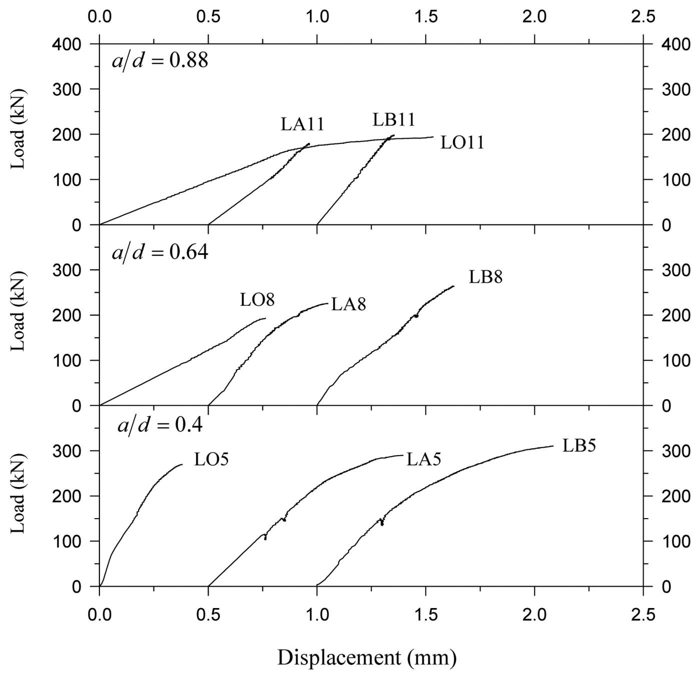

Fig. 3 Load versus displacement relationship of corbels

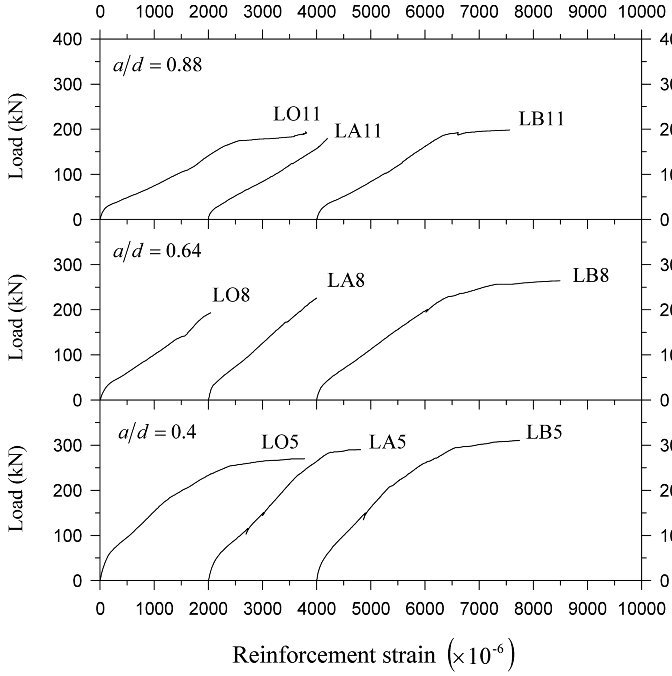

Fig. 4 Load versus reinforcement strain relationship of corbels

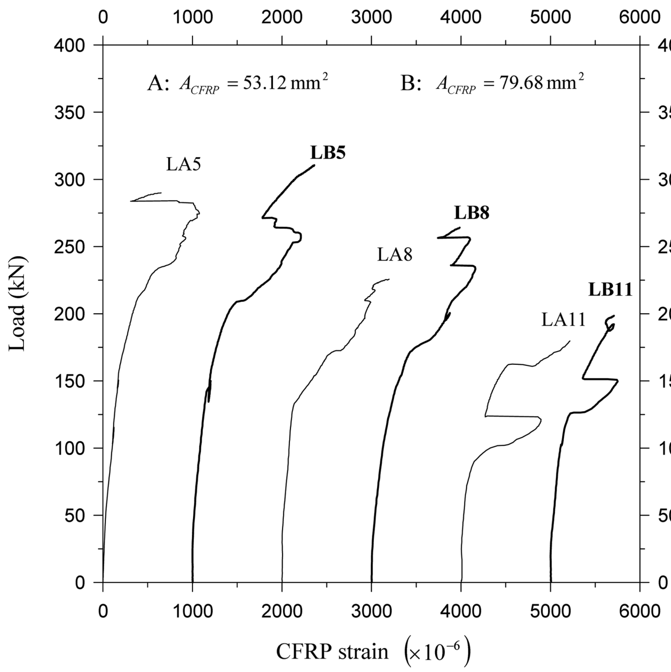

Fig. 5 Load versus CFRP strain relationship of corbels

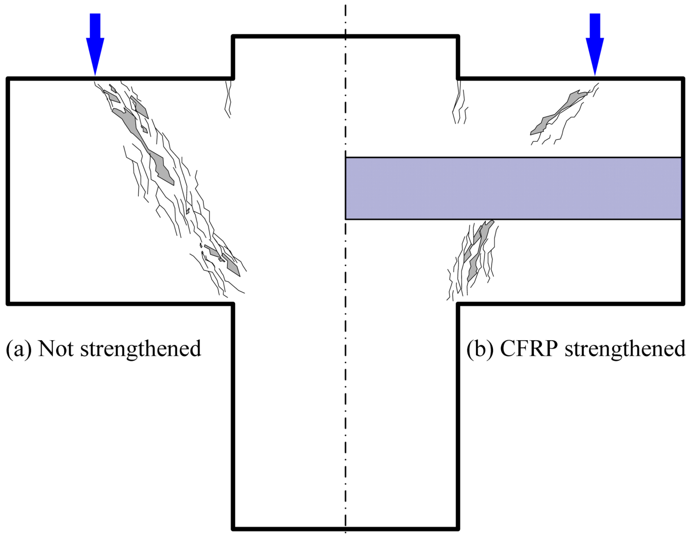

Fig. 6 Typical failures of corbels

greater effect on the ultimate load and displacement than for corbels with $a/d = 0.64$ and 0.88. The observed relationship between load and strain in the primary reinforcement of the corbels is shown in Fig. 4. For corbels with $a/d = 0.4$, the greater the A_{CFRP}, the greater is the ultimate strain in the primary reinforcement. However, for corbels with $a/d = 0.64$ and 0.88, the effect of CFRP, on the ultimate strain in the primary reinforcement, was not obvious (Fig. 4). The observed load versus CFRP strain relationship of corbels is shown in Fig. 5. The effect of A_{CFRP} on load versus CFRP strain relationship was unnoticed (Fig. 5).

A typical failure, for corbels not strengthened with CFRP, is shown on the left side of Fig. 6. The shear action in the corbel leads to compression, in the diagonal direction, and tension, in the perpendicular direction. Flexural cracks are formed, at about 40% of the ultimate load, and then diagonal cracks formed, at the middle of the corbel, due to the diagonal tension. As the load increases, flexural and diagonal cracks also develop. However, the formation of diagonal cracks did not cause the corbels to fail immediately. The concrete between the diagonal cracks constitutes a diagonal compression strut, which transfers the external shear, so the ultimate failure mode can be the diagonal compression failure, or the failure initiated by the yielding of the primary reinforcement. A typical failure of corbels strengthened with CFRP is shown on the right side of Fig. 6. The behavior of corbels, strengthened with CFRP, is similar to that of corbels that are not strengthened with CFRP, except that the diagonal cracks do not develop in the area covered by CFRP. Most cracks are restricted to the top and bottom of the corbels, as shown on the right side of Fig. 6.

3. Design model

According to the ACI Code (2008), corbels with $a/d \leq 1$ can be designed, using the provisions of section 11.8, and corbels with $1 < a/d \leq 2$ should be designed, using the strut-and-tie model, in Appendix A of the ACI Code (2008).

Table 6 Shear strength predicted by section 11.8 of the ACI Code

Specimen	a/d	A_{CFRP} (mm^2)	$V_{cv,calc}$ (kN)				
			Eq. (1)	Eq. (2)	Eq. (3)	Eq. (4)	Eq. (5)
LO5	0.40	0	215.66	136.93	97.05	100.70	206.26
LA5	0.40	53.12	215.66	136.93	97.05	100.70	206.26
LB5	0.40	79.68	215.66	136.93	97.05	100.70	206.26
LO8	0.64	0	134.79	136.93	97.05	100.70	206.26
LA8	0.64	53.12	134.79	136.93	97.05	100.70	206.26
LB8	0.64	79.68	134.79	136.93	97.05	100.70	206.26
LO11	0.88	0	98.03	136.93	97.05	100.70	206.26
LA11	0.88	53.12	98.03	136.93	97.05	100.70	206.26
LB11	0.88	79.68	98.03	136.93	97.05	100.70	206.26

3.1 ACI 11.8

According to the provisions of section 11.8, the shear strength of corbels shall not exceed the smallest value produced by the following equations

$$V_{cv,calc} = \frac{1}{a}\left[A_f f_f\left(d - \frac{A_y f_y}{1.7 f_c' b}\right) - N_c(h-d)\right] \tag{1}$$

$$V_{cv,calc} = \mu(A_s f_y + A_h f_{yh} - N_c) \tag{2}$$

$$V_{cv,calc} = 0.2 f_c' bd \tag{3}$$

$$V_{cv,calc} = (3.3 + 0.08 f_c')bd \tag{4}$$

$$V_{cv,calc} = 11bd \tag{5}$$

where $V_{cv,calc}$ is the predicted shear strength of corbels, A_f is the area of the flexural bars, $A_f = A_s - N_c/f_y$, A_s is the area of primary reinforcement, N_c is the horizontal tensile force, f_c' is the compressive strength of concrete, μ is the coefficient of friction, A_h is the area of the horizontal stirrup and f_{yh} is the yield strength of the horizontal stirrup.

The shear strengths predicted by section 11.8 of the ACI Code are shown in Table 6. For corbels with different values of a/d and A_{CFRP}, all of the predicted shear strengths are equal to 97.05 kN, as governed by Eq. (3), in section 11.8 of the ACI Code.

3.2 ACI strut-and-tie model

According to the strut-and-tie model of the ACI Code, the shear strength of corbels shall be calculated using with the smallest value for the strength of the struts, strength of the ties and strength of the nodal zones.

The strength of the struts, F_{ns}, based upon the strut-and-tie model of the ACI Code, can be calculated as follows

$$F_{ns} = f_{cu} A_c \tag{6}$$

where f_{cu} is the effective compressive strength of the concrete in the strut and shall be taken as

$$f_{cu} = 0.85\beta_s f_c' \tag{7}$$

where β_s is the strength coefficient. For f_c' not greater than 41.4 MPa and where the axis of the strut is crossed by layers of reinforcement (Fig. 7) to satisfy Eq. (8), β_s is taken as 0.75, β_s is taken as 0.4 for strut in tension member. In all other cases, β_s is taken as 0.6.

$$\sum \frac{A_{si}}{bs_i} \sin \gamma_i \geq 0.003 \tag{8}$$

where A_{si} is the total area of surface reinforcement, at spacing, s_i, in the i-th layer of reinforcement,

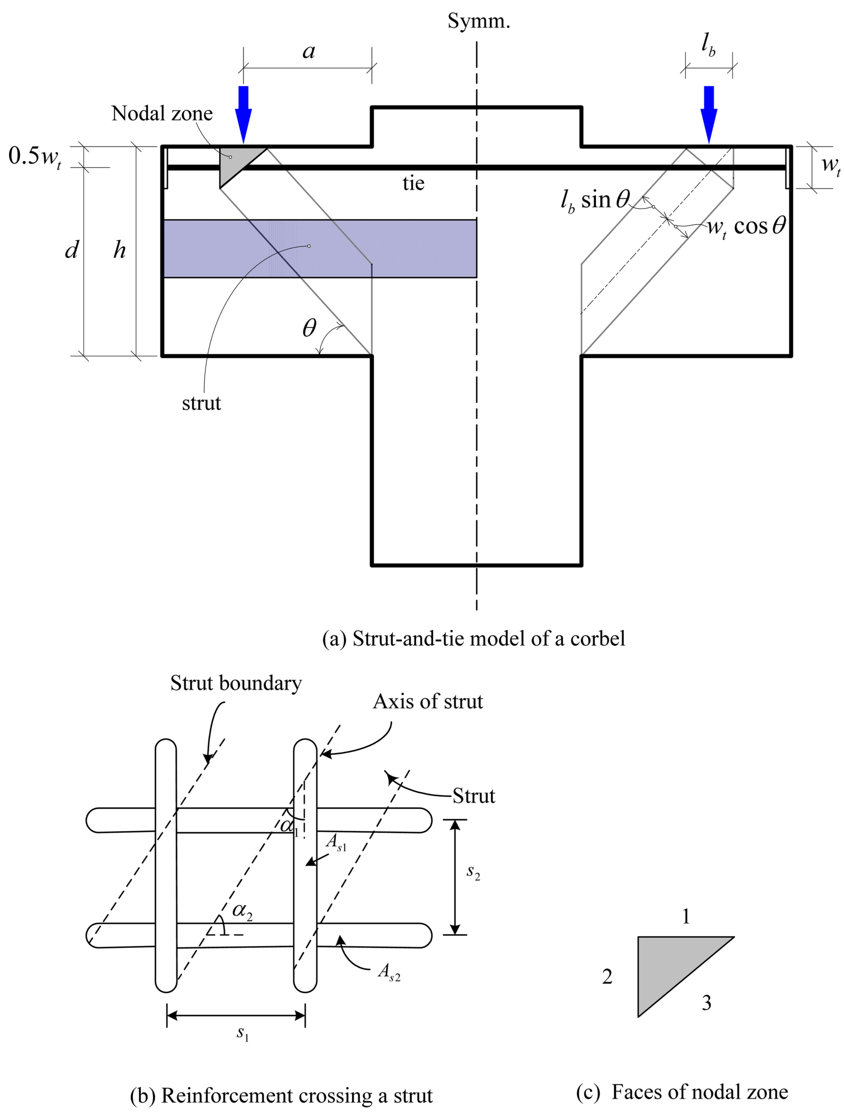

Fig. 7 Strut-and-tie model of the ACI Code

crossing a strut at an angle, γ_i, to the axis of the strut. It is intuitively assumed that A_{si} shall be taken as A_{CFRP}, in this study.

The cross-sectional area of the strut (A_c) shall be taken as

$$A_c = w_s b \tag{9}$$

where w_s is the width of strut. As shown in Fig. 7, w_s can be calculated as follows

$$w_s = w_t \cos\theta + l_b \sin\theta \tag{10}$$

where w_t is the effective tie width, l_b is the width of the bearing plate and θ is the inclined angle of strut (Fig. 7).

The shear strength of the corbel governed by the strength of the strut (V_{strut}), which can be calculated as

$$V_{strut} = F_{ns} \sin\theta \tag{11}$$

Table 7 shows the shear strength of the corbel, governed by the strength of the strut, for the strut-and-tie model of the ACI Code.

The strength of tie, F_{nt}, according to the strut-and-tie model of the ACI Code, shall be taken as

$$F_{nt} = A_s f_y \tag{12}$$

Table 7 Strength of struts predicted by strut-and-tie model of the ACI Code

Specimen	f_c' (MPa)	θ (°)	l_b (mm)	w_t (mm)	w_s (mm)	A_c (mm^2)	A_{CFRP} (mm^2)	γ_i (°)	$\sum\frac{A_{si}\sin\gamma_i}{bs_i}$	β_s	f_{cu} (MPa)	V_{strut} (kN)
LO5	25.88	53.1	50	50	70	10500	0	53.1	0	0.6	13.20	110.87
LA5	25.88	53.1	50	50	70	10500	53.12	53.1	0.0019	0.6	13.20	110.87
LB5	25.88	53.1	50	50	70	10500	79.68	53.1	0.0028	0.6	13.20	110.87
LO8	25.88	43.6	50	50	70.70	10603.45	0	43.6	0	0.6	13.20	96.52
LA8	25.88	43.6	50	50	70.70	10603.45	53.12	43.6	0.0016	0.6	13.20	96.52
LB8	25.88	43.6	50	50	70.70	10603.45	79.68	43.6	0.0024	0.6	13.20	96.52
LO11	25.88	36.5	50	50	69.94	10490.89	0	36.5	0	0.6	13.20	82.42
LA11	25.88	36.5	50	50	69.94	10490.89	53.12	36.5	0.0014	0.6	13.20	82.42
LB11	25.88	36.5	50	50	69.94	10490.89	79.68	36.5	0.0021	0.6	13.20	82.42

Table 8 Strength of ties predicted by strut-and-tie model of the ACI Code

Specimen	A_s (mm^2)	f_y (MPa)	θ (°)	V_{tie} (kN)
LO5	253.4	386	53.1	130.54
LA5	253.4	386	53.1	130.54
LB5	253.4	386	53.1	130.54
LO8	253.4	386	43.6	93.15
LA8	253.4	386	43.6	93.15
LB8	253.4	386	43.6	93.15
LO11	253.4	386	36.5	72.45
LA11	253.4	386	36.5	72.45
LB11	253.4	386	36.5	72.45

The shear strength of the corbel, governed by the strength of the tie (V_{tie}), can be calculated as

$$V_{tie} = F_{nt} \tan \theta \tag{13}$$

Table 8 shows the shear strength of the corbel, governed by the strength of the tie, for the strut-and-tie model of the ACI Code.

According to the strut-and-tie model of the ACI Code, the strength of the nodal zone, F_{nn}, shall be taken as follows

$$F_{nn} = f_{cn} A_n \tag{14}$$

where f_{cn} is the effective compressive strength of the concrete, in the nodal zone

$$f_{cn} = 0.85 \beta_n f_c' \tag{15}$$

where β_n is the strength coefficient. In nodal zones bounded by struts, or bearing areas, or both, β_n is taken as 1.0. In nodal zones anchoring one tie, β_n is taken as 0.80. In nodal zones anchoring two, or more ties, β_n is taken as 0.60.

The cross-sectional area of the nodal zones (A_n) shall be taken as the smaller of the area of the face of the nodal zone, on which the largest force, F_u, acts, taken perpendicular to the line of action of F_u and the area of a section through the nodal zone, taken perpendicular to the line of the resultant force on the section.

Table 9 Strength of nodal zone predicted by strut-and-tie model of the ACI Code

Specimen	f_c' (MPa)	β_n	V_1 (kN)	V_2 (kN)	V_3 (kN)	V_n (kN)
LO5	25.88	0.8	131.99	175.98	184.78	131.99
LA5	25.88	0.8	131.99	175.98	184.78	131.99
LB5	25.88	0.8	131.99	175.98	184.78	131.99
LO8	25.88	0.8	131.99	125.70	186.60	125.70
LA8	25.88	0.8	131.99	125.70	186.60	125.70
LB8	25.88	0.8	131.99	125.70	186.60	125.70
LO11	25.88	0.8	131.99	97.77	184.62	97.77
LA11	25.88	0.8	131.99	97.77	184.62	97.77
LB11	25.88	0.8	131.99	97.77	184.62	97.77

Table 10 Shear strength predicted by strut-and-tie model of the ACI Code

Specimen	V_{strut} (kN)	V_{tie} (kN)	V_n (kN)	$V_{cv,calc}$ (kN)
LO5	110.87	130.42	131.99	110.87
LA5	110.87	130.42	131.99	110.87
LB5	110.87	130.42	131.99	110.87
LO8	96.52	93.15	125.70	93.15
LA8	96.52	93.15	125.70	93.15
LB8	96.52	93.15	125.70	93.15
LO11	82.42	72.45	97.77	72.45
LA11	82.42	72.45	97.77	72.45
LB11	82.42	72.45	97.77	72.45

The shear strength of the corbel, governed by the strength of the nodal zone (V_n), is shown in Table 9. The shear strength of corbels, based on the strut-and-tie model, shall be taken as the smallest value of V_{strut}, V_{tie} or V_n (Table 10).

4. The SST model

Fig. 8 shows the loads acting on the corbel and the force transfer mechanisms of the SST model (Hwang *et al.* 2000, Lu *et al.* 2010). Considering the distances between force couples (Fig. 8), it is sufficiently accurate to express the following relationship between vertical and horizontal shears as

$$\frac{V_{cv}}{V_{ch}} \approx \frac{jd}{a} \tag{16}$$

where V_{cv} is the vertical shear force, V_{ch} is the horizontal shear force and jd is the length of the lever arm from the resultant compressive force, to the centroid of the flexural reinforcement. According to the linear bending theory, the lever arm, jd, can be estimated as

$$jd = d - kd/3 \tag{17}$$

where kd is the depth of the compression zone, at the section, and the coefficient, k, can be defined as

$$k = \sqrt{(n\rho_f)^2 + 2n\rho_f} - n\rho_f \tag{18}$$

where n is the modular ratio of elasticity and can be defined as

$$n = \frac{E_s}{E_c} \tag{19}$$

where E_s is the elastic modulus of the steel, E_c is the elastic modulus of the concrete and ρ_f is the ratio of flexural bar.

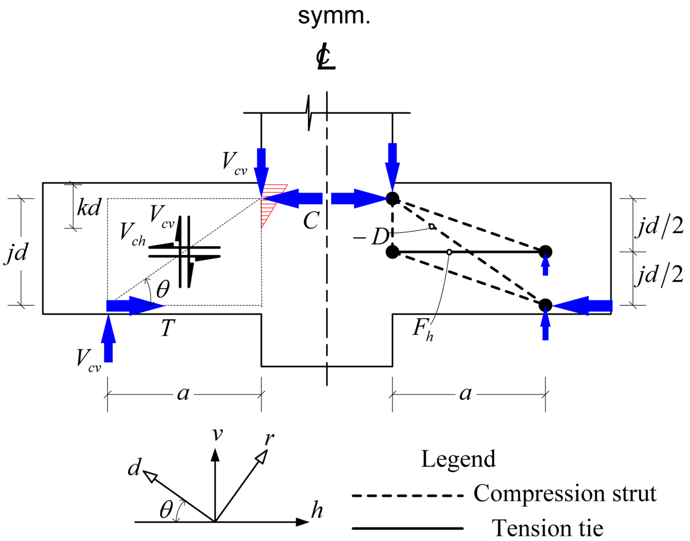

Fig. 8 SST model for internal forces (Lu *et al.* 2009)

Fig. 8 shows the proposed SST model, which is composed of diagonal and horizontal mechanisms (Hwang *et al.* 2000). The diagonal mechanism is a diagonal compression strut, whose angle of inclination, θ, is defined as (Hwang *et al.* 2000).

$$\theta = \tan^{-1}\left(\frac{jd}{a}\right) \tag{20}$$

The effective area of the diagonal strut, A_{str}, can be estimated as

$$A_{str} = t_s \times b \tag{21}$$

where t_s is the thickness of the diagonal strut. The thickness of the diagonal strut is dependent on its end condition, provided by the compression zone at the column face. It is intuitively assumed that (Hwang *et al.* 2000).

$$t_s = kd \tag{22}$$

The horizontal mechanism consists of one horizontal tie and two flat struts (Hwang *et al.* 2000). Since the CFRP wrapping is located in the middle of corbels, the cross-sectional area of CFRP is fully effective, when computing the area of the horizontal tie (A_{th}), i.e., $A_{th} = A_{CFRP}$.

According to Hwang and Lee (2002) and Lu *et al.* (2010), the diagonal compression strength of the corbel can be estimated as follows

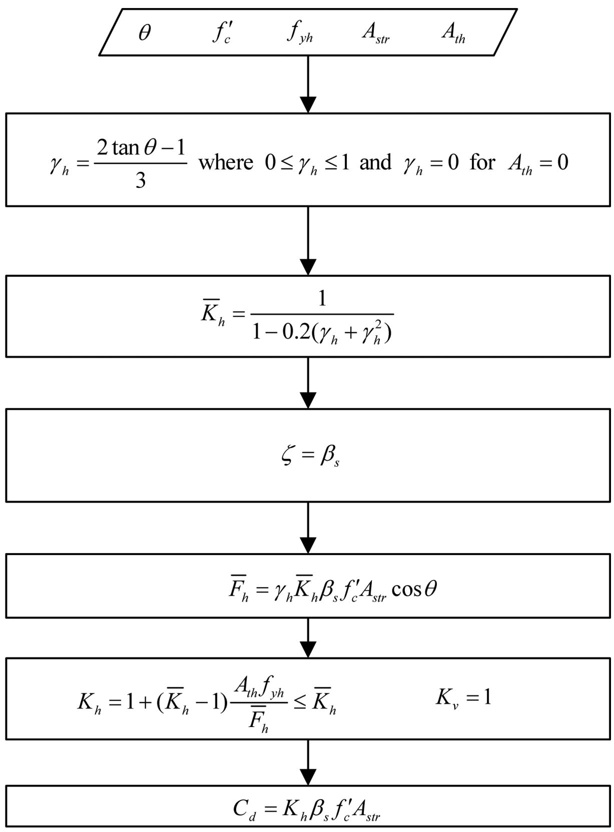

Fig. 9 Solution procedures for the SST model

$$C_d = (K_h + K_v - 1)\zeta f_c' A_{str} \tag{23}$$

where C_d is the predicted diagonal compression strength, K_h is the horizontal tie index, K_v is the vertical tie index and ζ is the softening coefficient of concrete in compression. In the absence of a vertical tie, K_v is equal to unity. According to this study's experimental observation (Fig. 6), the CFRP restricts the development of diagonal cracks, allowing the strut to increase its resistance to diagonal compression. It is intuitively assumed that $\zeta = \beta_s$ in this study. Thus, Eq. (23) is simply rewritten as

$$C_d = K_h \beta_s f_c' A_{str} \tag{24}$$

The solution algorithm for C_d is summarized in Fig. 9. The predicted shear strength of the corbel can be determined as follow

$$V_{cv,calc} = C_d \sin\theta \tag{25}$$

The shear strengths of the corbels, predicted by the SST model, are shown in Table 11.

Table 11 Shear strength predicted by SST model

Specimen	a/d	f_c' (MPa)	θ (°)	A_{str} (mm²)	A_{th} (mm²)	f_h (MPa)	β_s	K	$V_{cv,calc}$ (kN)
LO5	0.40	25.88	65.4	7044	0	0	0.6	1.00	99.48
LA5	0.40	25.88	65.4	7044	53.12	150	0.6	1.07	106.45
LB5	0.40	25.88	65.4	7044	79.68	313	0.6	1.22	121.29
LO8	0.64	25.88	53.8	7044	0	0	0.6	1.00	88.28
LA8	0.64	25.88	53.8	7044	53.12	276	0.6	1.07	94.60
LB8	0.64	25.88	53.8	7044	79.68	227	0.6	1.09	96.08
LO11	0.88	25.88	44.8	7044	0	0	0.6	1.00	77.12
LA11	0.88	25.88	44.8	7044	53.12	281	0.6	1.05	81.06
LB11	0.88	25.88	44.8	7044	79.68	163	0.6	1.04	80.55

Table 12 Comparison of tested and calculated shear strength of corbels

Specimen	a/d	f_c' (MPa)	θ (°)	A_{CFRP} (mm²)	$V_{cv,test}$ (kN)	$V_{cv,test}/V_{cv,calc}$		
						ACI 11.8	ACI Strut-and-tie	SST
L05	0.40	25.88	65.4	0	134.8	1.39	1.22	1.36
LA5	0.40	25.88	65.4	53.12	144.6	1.49	1.31	1.36
LB5	0.40	25.88	65.4	79.68	154.8	1.60	1.40	1.28
L08	0.64	25.88	53.8	0	98.0	1.01	1.04	1.09
LA8	0.64	25.88	53.8	53.12	112.7	1.16	1.21	1.19
LB8	0.64	25.88	53.8	79.68	131.8	1.36	1.42	1.37
L011	0.88	25.88	44.8	0	95.8	0.99	1.34	1.26
LA11	0.88	25.88	44.8	53.12	89.7	0.92	1.24	1.11
LB11	0.88	25.88	44.8	79.68	99.2	1.02	1.37	1.23
					AVG	1.22	1.28	1.25
					COV	0.20	0.09	0.08

5. Experimental verification

Test results for nine corbels were used to verify the analytical models. Table 12 compares the measured failure loads with the predictions, using the provisions in section 11.8 of the ACI Code, the strut-and-tie model of the ACI Code and the SST model. The accuracy of these analytical models is gauged, in terms of a strength ratio, which is defined as the ratio of the measured strength to the calculated strength. The comparisons show that both the strut-and-tie model and the SST model accurately predict the shear strength of the reinforced concrete corbels, strengthened with CFRP. The comparisons also show that the shear strength of the reinforced concrete corbels, strengthened with CFRP, might be over-estimated by the design provisions in section 11.8 of the ACI Code.

6. Conclusions

A total of nine reinforced concrete corbels were tested, in this study. Six were externally strengthened with CFRP, in the horizontal direction. The test results were compared with the provisions in section 11.8 of the ACI Code, the strut-and-tie model of the ACI Code and the SST model. Based on test results and comparison with the predictions of these analytical methods, the following conclusions are drawn:

1. The shear strength of corbels with shear span-to-effective depth ratios (a/d) of 0.4 and 0.64 increases, as the cross-sectional area of the CFRP (A_{CFRP}) is increased. However, the effect of A_{CFRP}, on the shear strength of corbels, is not obvious, for the condition a/d = 0.88 (Table 5).
2. CFRP wrapping, in the horizontal direction has a greater effect on the ultimate load and displacement of corbels with a/d = 0.4 than on corbels with a/d = 0.64 and 0.88 (Fig. 3).
3. Both the strut-and-tie model in Appendix A of the ACI Code, and the SST model can accurately predict the shear strength of reinforced concrete corbels, strengthened with CFRP (Table 12).

Acknowledgements

This research study was partially sponsored by the National Science Council of the Republic of China under Project NSC 99-2221-E-163-002. The authors would like to express their gratitude for the support. Susanna Yang (secretary of the Department of Interior design at China University of Technology) kindly improved the English in this paper.

References

American Concrete Institute (2008), *Building code requirements for structural concrete (ACI 318-08) and Commentary (ACI 318R-08),* Farmington Hills, Mich.

Elwan, S.K. and Rashed, A.S. (2011), "Experimental behavior of eccentrically load R.C. short columns strengthened using CFRP wrapping", *Struct. Eng. Mech.*, **39**(2), 207-221.

Fattuhi, N.I. (1994), "Reinforced corbels made with plain and fibrous concrete", *ACI Struct. J.*, **91**(5), 530-536.

Foster, S.J., Powell, R.E. and Selim, H.S. (1996), "Performance of high-strength concrete corbels", *ACI Struct. J.*, **93**(5), 555-563.

Hwang, S.J., Lu, W.Y. and Lee, H.J. (2000), "Shear strength prediction for reinforced concrete corbels", *ACI Struct. J.*, **97**(4), 543-552.

Hwang, S.J. and Lee, H.J. (2002), "Strength prediction for discontinuity regions failing in diagonal compressions by softened strut-and-tie model", *J. Struct. Eng.-ASCE*, **128**(12), 1519-1526.

Her, G.J. (1990), *A study of reinforced high-strength concrete corbels*, Master's Thesis, Department of Construction Engineering, National Taiwan University of Science and Technology, Taipei, Taiwan (in Chinese).

Kriz, L.B. and Raths, C.H. (1965), "Connections in precast concrete structures - strength of corbels", *PCI J.*, **10**(1), 16-61.

Li, Y.F., Lin, C.T. and Sung, Y.Y. (2003), "A constitutive model for concrete confined with carbon fiber reinforced plastics", *Mech. Mater.*, **35**(3), 603-619.

Lu, W.Y. and Lin, I.J. (2009), "Behavior of reinforced concrete corbels", *Struct. Eng. Mech.*, **33**(3), 357-371.

Lu, W.Y., Lin, I.J. and Hwang, S.J. (2009), "Shear strength of reinforced concrete corbels", *Mag. Concrete Res.*, **61**(10), 807-813.

Lu, W.Y., Hwang, S.J. and Lin, I.J. (2010), "Deflection prediction for reinforced concrete deep beams", *Comput. Concrete*, **7**(1), 1-16.

Mattock, A.H., Chen, K.C. and Soongswang, K. (1976), "The behavior of reinforced concrete corbels", *PCI J.*, **21**(2), 52-77.

Russo, G., Venir, R., Pauletta, M. and Somma, G. (2006), "Reinforced concrete corbels-shear strength model and design formula", *ACI Struct. J.*, **103**(1), 3-10.

Shuraim, A.B. (2011), "Efficacy of CFRP configurations for shear of RC beams: experimental and NLFE", *Struct. Eng. Mech.*, **39**(3), 361-382.

Wong, F.J. and Vecchio, F.J. (2003), "Towards modeling of reinforced concrete members with externally bonded fiber-reinforced polymer composites", *ACI Struct. J.*, **100**(1), 47-55.

Yong, Y.K. and Balaguru, P. (1994), "Behavior of reinforced high-strength-concrete corbels", *J. Struct. Eng.-ASCE*, **120**(4), 1182-1201.

CC

Notations

a = shear span, measured from the center of the support to the face of the column
A_b = area of an individual bar
A_c = cross-sectional area of the strut
A_{CFRP} = cross-sectional area of CFRP
A_f = area of flexural bars
A_h = area of the horizontal stirrups
A_n = cross-sectional area of the nodal zones
A_s = area of primary reinforcement
A_{si} = total area of surface reinforcement at spacing s_i
A_{th} = area of the horizontal tie
A_{str} = effective area of the diagonal strut
b = width of corbel
C = resultant compressive force at section due to flexure
C_d = predicted diagonal compression strength
d = effective depth of corbel
d_b = nominal diameter of bar
E_c = elastic modulus of the concrete
E_s = elastic modulus of the steel
f_c' = compressive strength of concrete
f_{cn} = effective compressive strength of the concrete in the nodal zone
f_{cu} = effective compressive strength of the concrete
f_h = average tensile stress in the horizontal tie
F_{nt} = strength of tie based on the strut-and-tie model of the ACI Code
f_u = ultimate tensile strength of steel
f_y = yield strength of steel
f_{yh} = yield stress of the horizontal stirrup
F_h = tension force in the horizontal tie (positive for tension)
$\overline{F}_h$ = the balanced amount of the horizontal tie force
F_{nn} = strength of nodal zones based on the strut-and-tie model of the ACI Code
F_{ns} = strength of strut based on the strut-and-tie model of the ACI Code
F_{yh} = yielding force of the horizontal ties
h = overall depth of corbel
j, k = coefficients
K_h = the horizontal tie index
$\overline{K}_h$ = horizontal tie index with sufficient horizontal reinforcement
K_v = the vertical tie index
jd = distance of the lever arm from the resultant compressive force to the centroid of the flexural tension reinforcement
kd = depth of compression zone at the section
l_b = width of the bearing plate
n = modular ratio of elasticity
= E_s/E_c
N_c = horizontal tensile force

P_u = ultimate load measured in the test
T = tension in the flexural bars
t_s = depth of the diagonal strut
V_{ch}, V_{cv} = horizontal and vertical shear forces, respectively
$V_{cv,calc}$ = predicted shear strength of corbels
$V_{cv,test}$ = the shear strength of corbels measured in the test
V_{strut} = shear strength of corbel governed by the strength of strut
V_{tie} = shear strength of corbel governed by the strength of tie
w_s = width of strut
w_t = effective tie width
β_n, β_s = strength coefficient
γ_h = fraction of horizontal shear transferred by the horizontal tie in the absence of the vertical tie
θ = inclined angle of strut
ρ = ratio of the primary reinforcement of corbels
ρ_f = ratio of the flexural bar
ζ = softening coefficient of concrete in compression
μ = friction coefficient
λ = coefficient for type of concrete